13th Australasian Fluid Mechanics Conference
Monash University, Melbourne, Australia
13-18 December 1998

CONVECTIVELY DRIVEN EXCHANGE FLOW IN A SILL-ENCLOSED BASIN

Tim FINNIGAN and Greg IVEY

Centre for Water Research
University of Western Australia, Nedlands, WA, AUSTRALIA

ABSTRACT

We consider the unsteady response of a semi-enclosed basin to a destabilising buoyancy flux which is suddenly imposed at the surface. When the basin is connected to a large homogeneous reservoir, then the forcing results in a lateral density gradient and an associated mean flow into the basin near the surface. An underlying return flow is required and the resulting exchange may be controlled in a hydraulic sense by a sill which separates the basin and reservoir.

The processes by which the basin circulation proceeds from an initial rest state to a steady circulation state are explained using scaling methods and laboratory experiments. It appears that the dominant balance is initially between the unsteady and buoyancy terms but changes smoothly to a quasi-steady inertia-buoyancy balance once a mean flow is established. The basin continues to adjust under this regime until a final steady state is reached. At steady-state the inertia-buoyancy balance is modified to accomodate the effects of turbulent fluxes and mixing within the basin. The result ties together the internal hydraulic control at the sill and the interior basin conditions, and allows the specification of mean submaximal exchange fluxes given the forcing strength and system geometry.

INTRODUCTION

Exchange of fluid through a constriction between two sources of differing density is a topic which has generated significant interest since Stommel and Farmer (1953) first proposed a controlling mechanism for estuarine flows. Many studies have been concerned with the details of transport and stratification within the constriction itself. Relatively few studies have focussed on the relationship between the flow through the constriction and conditions within the adjoining water bodies. We present a study which investigates this relationship where the system concerned is comprised of an infinite reservoir which communicates with a basin of limited extent.

The two fluid bodies are separated by a shallow sill while the width of the system is uniform. In order for an exchange flow to persist, a density gradient across the sill must be maintained by either a source or sink of buoyancy within the basin. In our case, this is achieved by applying a uniform buoyancy flux directed upwards at the surface of the basin. The response includes a lateral current moving into the basin near the surface and a deeper compensating return flow (see Figure 1). Geophysical examples of such systems include the Red and Mediterranean Seas, where the combined effect of evaporation and cooling produces the destabilising buoyancy flux at the surface (Phillips, 1966). Some Arctic fjords are subjected to similar forcing conditions when either cooled at the surface or when a growing layer of sea-ice ejects brine and hence reduces buoyancy near the surface (Møller, 1984).

Starting with homogeneous density distributions in both basin and reservoir, we investigate through scaling of the governing equations and laboratory experiments, the unsteady response of the system when the surface buoyancy flux condition is suddenly applied and then held constant. The adjustment under these conditions is a model for what happens in natural systems that are exposed to rapid climatic changes, the onset of freezing, or large seasonal climate fluctuations. An equilibrium is established at steady-state between an internal hydraulic control at the sill and interior mixing conditions within the basin.

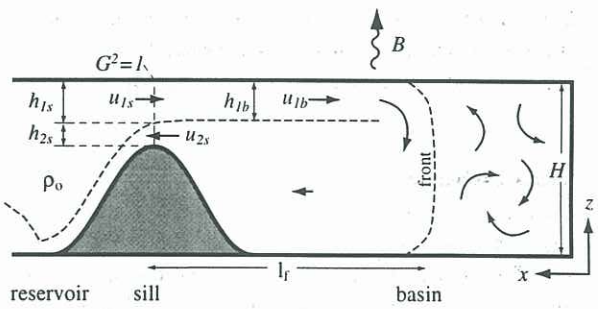

Figure 1: Schematic diagram of basin-sill-reservoir system. The system is shown here undergoing basin adjustment with the exchange front moving from left to right.

EXPERIMENTAL METHOD

The laboratory experiments were performed in a rectangular tank with dimensions 2000x100x500mm. A sill was located 250mm from one end and the surface buoyancy flux was applied within the resulting smaller enclosure, having the configuration shown in Figure 1. A thermally generated buoyancy flux, B was established by altering the temperature of a copper plate acting as the basin surface. A manifold behind the plate was flushed with water to produce a temperature difference $\Delta T = |T_{ambient} - T_{manifold}|$ and therefore generate a buoyancy flux through the plate. Five experiments with different values of B were conducted (Table 1).

Experiment	ΔT (^oC)	$B \times 10^6$ ($m^2 s^{-3}$)
1	10	1.2
2	17.5	6.5
3	25	9.2
4	4	0.6
5	32.5	17

Table 1: Experimental buoyancy flux B values.

Velocity measurements within a vertical plane oriented along the basin were obtained through particle image velocimetry (PIV). Buoyancy measurements were obtained using fast-response thermistors which periodically profiled the basin depth at six lateral locations. Temperature time-series were also recorded at fixed depths when the flow was at steady-state.

Figure 2 shows the instantaneous measured velocity and buoyancy fields at three different times during a typical experiment. At each time the panels labelled i show the two-dimensional velocity field obtained by PIV and the panels labelled ii show the buoyancy field as measured by vertical thermistor traces at six horizontal locations. The dynamic balances existing in the flow at each time are discussed in the following section. A more detailed description of the experiments is given by Finnigan and Ivey (1998).

BASIN FLOW DYNAMICS

Laboratory results indicated that the system adjusts through two identifiable unsteady states before reaching the final steady state. We describe these as follows.

Initial Exchange

During the initial state, the destabilising buoyancy flux generates turbulent convection within the basin and the resulting lateral buoyancy gradient across the sill is associated with acceleration of an exchange flow between the basin and reservoir. This is clearly seen in Figure 2ai. At the sill the response is predominantly horizontal and a balance between the unsteady terms and the buoyancy terms in the vorticity equation leads to,

$$\frac{\partial}{\partial z}\left(\frac{\partial u}{\partial t}\right) \sim \frac{\partial b}{\partial x}, \qquad (1)$$

where t represents time, buoyancy is defined as $b = (\rho - \rho_o)/\rho_o$ and the remaining symbols are as defined in Figure 1. A simple heat budget in the sill region suggests that the time dependent buoyancy is given by $b \sim Bt/h$, which when combined with (1) leads to,

$$u \sim \frac{Bt^2}{l}, \qquad (2)$$

where h is the sill depth and l represents the horizontal scale of the accelerating current. This relationship is valid until non-linear inertia terms become comparable to the driving buoyancy term or,

$$\frac{\partial}{\partial z}\left(u\frac{\partial u}{\partial x}\right) \sim \frac{\partial b}{\partial x}, \qquad (3)$$

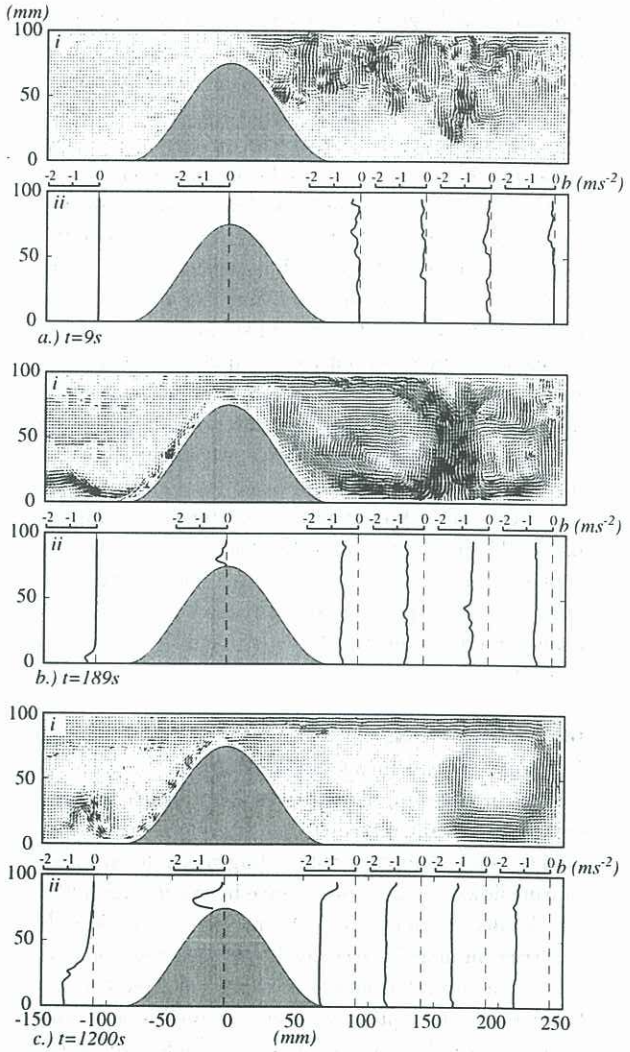

Figure 2: Measured velocity (i) and buoyancy (ii) fields for experiment 3 at three different times. Similar dynamics were observed in the other four experiments although with different time and velocity scales which are dependent on B.

which, when combined with (2), leads to a timescale,

$$t_t \sim \frac{l^{2/3}}{B^{1/3}} \sim \frac{l}{(Bl)^{1/3}}. \qquad (4)$$

For times greater than t_t a new balance exists. For the experiments described here t_t is on the order of $30s$ when l is taken to be the length of the current when it has extended beyond the sill region.

Basin Adjustment

Once established, the exchange flow begins to penetrate into the basin while a convectively dominated region remains towards the closed end of the basin (see Figures 1 and $2bi$). As a result of the surface forcing, the surface layer exhibits a decrease in buoyancy with distance into the basin. At some location, l_f, the buoyancy in the surface flow equals that in the end region and the locally neutral conditions allow the surface current to descend and turn back towards the external reservoir, thus completing the exchange circuit. The buoyancy of the fluid in the end region, $b \sim Bt/H$, is continually decreasing with time as the fluid is convectively mixed over the entire basin depth, H. The front of the exchange flow is thus forced to progress further along the basin in order for the surface current to lose sufficient buoyancy to become locally neutral.

Assuming the velocity is slowly varying as the front progresses, we may postulate a quasi-steady inertia-buoyancy balance within the surface current,

$$u_{1b} \sim (bh_{1b})^{1/2}, \qquad (5)$$

where the subscript $1b$ refers to the upper layer within the basin (Figure 1). With the front located at l_f conservation of buoyancy requires $Bl_f \sim u_{1b}h_{1b}b$ which combines with (5) giving,

$$u_{1b} \sim (Bl_f)^{1/3}, \qquad (6)$$

and,

$$b \sim \frac{(Bl_f)^{2/3}}{h_{1b}}, \qquad (7)$$

which represents the buoyancy of the surface layer at l_f, and identically, the relative buoyancy between the layers at the sill crest. The relations (6) and (7) are analogous to the scaling results implied by Phillips' (1966) similarity formulation for steady flow in the Red Sea.

At l_f the buoyancy of the surface current equals that in the end region which suggests,

$$l_f(t) \sim B^{1/2}t^{3/2}\left(\frac{h_{1b}}{H}\right)^{3/2}, \qquad (8)$$

giving the location of the front, l_f at time, t. A curve representing (8) is shown in Figure 3 along with measured values from the experiments. The results tend

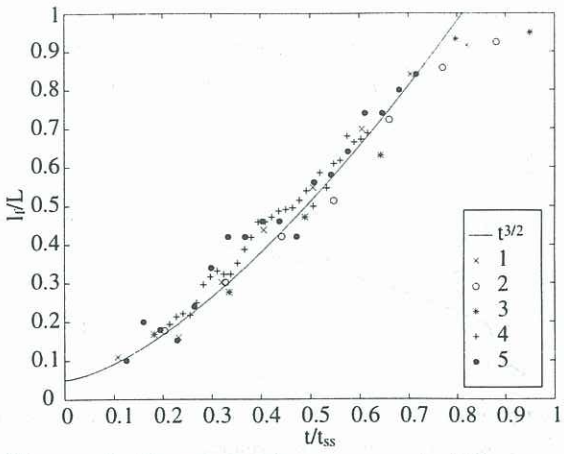

Figure 3: Experimental measurement of the location of the front compared with the scaling prediction of equation (8).

to support the scaling arguments except when the front nears the end-wall of the basin ($l_f \approx L$) and experiences some interference.

The velocity of the front is given by,

$$u_f = \frac{dl_f}{dt} \sim B^{1/2}t^{1/2}\left(\frac{h_{1b}}{H}\right)^{3/2}, \qquad (9)$$

which indicates that the acceleration of the front decreases as it moves along the length of the basin.

The surface layer velocity is found by combining (6) and (8),

$$u_{1b} \sim \left[Bt\left(\frac{h_{1b}}{H}\right)\right]^{1/2}. \qquad (10)$$

The scaling described above should be valid until the front reaches the end wall of the basin and $l_f = L$. The time of this occurrence is, from (8),

$$t_{ss} \sim L^{2/3}B^{-1/3}\left(\frac{H}{h_{1b}}\right) \qquad (11)$$

which is also the time of transition into the steady-state regime, hence the subscript ss. For comparison, this time is of the order of $500s$ for the experiments described here.

Steady State

At steady-state the velocity and buoyancy are expected to obey (6) and (7) except with l_f replaced by L.

Process Summary

The procession of the flow through the three stages described here is summarised in Figure 4 where the velocity at the sill, according to our scaling arguments, is shown as three separate curves. A transition from one balance to the next occurs where the curves intersect and the dark line indicates the path the system follows through the three stages. The velocity

and time scales in the figure are normalised by the steady-state values and the sill velocity is expressed as $u_{1s} = u_{1b}h_{1b}/h_{1s}$ (a two-layer assumption in the near sill region).

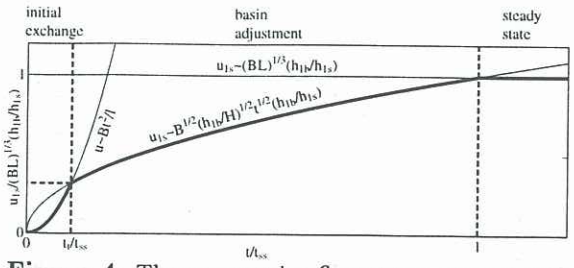

Figure 4: Three successive flow states, represented here by expressions for sill velocity, u_{1s}.

SILL-BASIN RELATIONSHIP

The internal hydraulic control at the sill crest isolates the sill and basin flows from reservoir conditions. However, mixing in the basin has a direct effect on the control condition and is therefore subjected to feedback which requires a sill-basin equilibrium at steady-state. The sill-basin coupling may be explored by combining the critical condition at the sill,

$$G^2 = \frac{u_{1s}^2}{bh_{1s}} + \frac{u_{2s}^2}{bh_{2s}} = 1, \qquad (12)$$

(Armi, 1986) with scaling results for mean flow parameters (u, b). Coefficients β and γ may be added to the left sides of equations (6) and (7) respectively before substituting the equalities into (12). Noting that $h = h_{1s} + h_{2s}$ and $u_{1s}h_{1s} = u_{2s}h_{2s}$ at the sill, we find,

$$\beta = \left(\frac{(h-h_{1s})^3}{(h-h_{1s})^3 + h_{1s}^3}\right)^{1/3} = \gamma^{-1}. \qquad (13)$$

If h_{1s} is known then the surface layer velocity at the sill may be calculated as $u_{1s} = \beta(BL)^{1/3}(h_{1b}/h_{1s})$ and the buoyancy difference between the counter flowing layers at the sill found from $b = \gamma(BL)^{2/3}/h_{1b}$. The upper layer depth (h_{1b}) a short distance into the basin may be eliminated from these relations by relating it to h_{1s} using hydraulic theory (Baines, 1995).

Equation (13) is plotted in Figure 4 which demonstrates that weak interior mixing tends to favour more submaximal flows ($\beta \ll 0.562$) and a deep interface level at the sill, while strong interior mixing drives the exchange towards the maximal limit with an interface depth $h_{1s} = 0.625h$ (Farmer and Armi, 1986). When the latter condition occurs the basin is said to be "overmixed" (Stommel and Farmer, 1953). The experimental results shown in Figure 5 indicate that the exchange becomes increasingly submaximal with increasing buoyancy forcing. Mixing and stratification do not increase proportionately and the coupling is therefore non-linear. In nature, other sources of energy may be available to either enhance or inhibit mixing. Despite this, the sill exchange and basin mixing always co-adjust to maintain equilibrium.

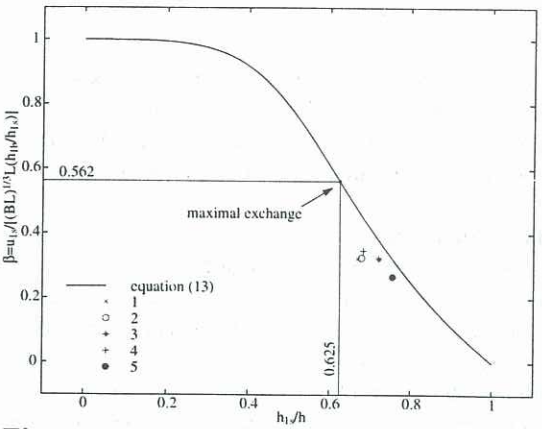

Figure 5: Sill-basin relationship (13) and measured values of β and h_{1s} for each experiment (symbols).

CONCLUSIONS

Scaling methods in comparison with laboratory experiments were used to describe the processes by which a suddenly forced sill-enclosed basin adjusts towards a steady-state. By combining scaling results with the hydraulic control condition we were able to explore the coupling between the exchange at the sill and basin interior mixing.

REFERENCES

ARMI, L., "The hydraulics of two flowing layers with different densities", *Journal of Fluid Mechanics,* **163**, 27-58, 1986.

BAINES, P.G., "Topographic effects in stratified flows", Cambridge University Press, pp 133-163, 1995.

FARMER, D.M. and ARMI, L., "Maximal two-layer exchange over a sill and through the combination of a sill and contraction with net barotropic flow", *Journal of Fluid Mechanics,* **164**, 53-76, 1986.

FINNIGAN, T.D. and IVEY, G.N., "Submaximal exchange between a convectively forced basin and a large reservoir", *Journal of Fluid Mechanics,* in press, 1998.

MØLLER, J.S., "Hydrodynamics of an Arctic fjord", *Technical Report, Institute of Hydrodynamics and Hydraulic Engineering, Technical University of Denmark, Lyngby,* Series Paper 34, 1984.

PHILLIPS, O.M., "On turbulent convection currents and the circulation of the Red Sea", *Deep-Sea Research,* **13,** 1149-1160, 1966.

STOMMEL, H. and FARMER, H.G., "Control of salinity in an estuary by a transition", *Journal of Marine Research,* **12,** 13-20, 1953.